Smart Structures and Systems, *Vol. 21, No. 5 (2018) 677-686*
DOI: https://doi.org/10.12989/sss.2018.21.5.677

Damage identification of vehicle-track coupling system from dynamic responses of moving vehicles

Hong-Ping Zhu[a], Ling Ye[b], Shun Weng[*] and Wei Tian[c]

School of Civil Engineering and Mechanics,
Huazhong University of Science and Technology, Wuhan 430074, China

(Received December 26, 2017, Revised March 22, 2018, Accepted March 25, 2018)

Abstract. The structural responses are often used to identify the structural local damages. However, it is usually difficult to gain the responses of the track, as the sensors cannot be installed on the track directly. The vehicles running on a track excite track vibration and can also serve as response receivers because the vehicle dynamic response contains the vibration information of the track. A damage identification method using the vehicle responses and sensitivity analysis is proposed for the vehicle-track coupling system in this paper. Different from most damage identification methods of vehicle-track coupling system, which require the structural responses, only the vehicle responses are required in the proposed method. The local damages are identified by a sensitivity-based model updating process. In the vehicle-track coupling system, the track is modeled as a discrete point supported Euler-Bernoulli beam, and two vehicle models are proposed to investigate the accuracy and efficiency of damage identification. The measured track irregularity is considered in the calculation of vehicle dynamic responses. The measurement noises are also considered to study their effects to the damage identification results. The identified results demonstrate that the proposed method is capable to identify the local damages of the track accurately in different noise levels with only the vehicle responses.

Keywords: vehicle-track coupling system; sensitivity-based method; damage identification

1. Introduction

Nowadays, the vehicle-track system is popularly used in public transportation system. The track is vulnerable to age and deteriorate in practical application. Therefore, it is significant to maintain a health condition of the track to ensure its structural completeness and work efficiency. It is known that damages in track will change the structural physical properties, such as stiffness, mass and boundary conditions, which implies these properties can be selected as indices for damage identification. The structural damage identification using dynamic responses and dynamic characteristic parameters has gained increasing attention in civil and mechanical engineering in the past few decades (He *et al*. 2017, Zhu *et al*. 2018).

Masses of damage identification methods have been proposed in many literatures (Alvandi *et al*. 2006, Fan *et al*. 2010, Ni *et al*. 2010, Ni *et al*. 2012, Feng *et al*. 2017) to research the vehicle-track system. They are frequently to be found for the vehicle parameter identification, axle force identification and structural damage identification. Deng *et al* (2009) and Kraft *et al*. (2016) used the dynamic responses to cope with the vehicle parameter identification. The dynamic response and characteristic parameters are used to identify the axle force between the vehicle and track by Gonzale *et al*. (2008), Chen *et al*. (2009) and Vikram *et al*. (2010). They are also utilized for structural damage identification of vehicle-track system in many other literatures.

Majumder *et al*. (2003) proposed a time domain approach for damage identification in beam structures using vibration data. Bilello *et al*. (2004) considered the passage of a moving mass over a damaged beam both theoretically and experimentally. In these literatures, the vehicle was treated as a concentrated mass, which is inaccurate as the vehicle is the main external excitation for the track. Afterwards, Bu *et al*. (2006) presented a method to identify the local damages of the bridge deck that subject to a moving vehicle. Lu *et al*. (2007) proposed a response sensitivity based method to identify the local damages of a beam structure. Zhu *et al*. (2007) provided similar numerical studies, which emphasizes the importance of bridge-vehicle interaction based damage detection in concrete bridges. Vikram *et al*. (2010) experimentally monitored the evolution of a crack in a beam using beam-vehicle interaction response signals, to identify the progressively increasing crack-depth ratios. Zhan *et al*. (2010) applied the dynamic responses of railway bridges for damage identification. Kong *et al*. (2014) detected and located damage of an experimental bridge model using Hilbert-Huang transform of transient vibration data.

∗Corresponding author, Associate Professor
E-mail: wengshun@hust.edu.cn
[a] Professor
E-mail: hpzhu@hust.edu.cn
[b] Ph.D. Student
E-mail: yeling0310@hust.edu.cn
[c] Master Student
E-mail: tianwei@hust.edu.cn

ISSN: 1738-1584 (Print), 1738-1991 (Online)

In most previous works, the track responses were used to identify the damages of the vehicle-track system. In the practical civil structures, the responses of the track were difficult to measure as the sensors are usually not allowed to be installed on the track directly. It is important to develop a new approach for the track damage identification with no instrumentation installed on the track.

For that goal, this paper proposed a method for damage identification of the track using only the vehicle responses. For vehicle-track coupling system, the movement of the vehicle will make the track in vibration. Relatively, the vibration of the track will lead to the motion of the vehicle. It means that the motion of the vehicle is affected by the change of the physical properties of the track. As a result, the response of the vehicle can be used to yield the physical properties of the track. That's the key idea for damage identification of the track using the dynamic response of the passing vehicle. A detailed time-domain model is developed for the vehicle-track coupling system. The track vertical profile irregularity is considered in this coupling model. The dynamic responses for the coupling system are calculated by the Newmark direct integration method. The response sensitivities with respect to the damage indices of the element are calculated to indicate the searching direction. Using the difference between the measured acceleration responses of the vehicle and the computed ones as a minimization criterion, the damage identification is performed by the least-squares method. A numerical vehicle-track system is employed to validate the accuracy of the proposed method. In the numerical analysis, the influence of measurement noise on the analysis results is discussed. For the degrees of freedom (DOFs) of the vehicle are much less than the DOFs of the track, the size of the sensitivity equations is reduced when the responses of the vehicle is chosen. Therefore, the proposed method is time-saving compared with the approaches using structural responses.

2. Dynamic responses analysis of the vehicle-track coupling system

The dynamic model of the vehicle-track coupling system is composed of a vehicle and a track, which are constrained by the interaction force and the displacement compatibility between them. To analyze the dynamic responses of the vehicle-track coupling system, the dynamic responses of the track and the vehicle, the interaction force, and the track irregularity need to be calculated.

2.1 Dynamic responses analysis of the track

The track model is shown in Fig. 1. It is modeled as a discrete point supported Euler-Bernoulli beam with N elements in the finite element model. The vibration equation of the track is written as

$$M_r\ddot{y}_r + C_r\dot{y}_r + K_r y_r = N_r^T F_{rv} \tag{1}$$

where M_r, C_r, and K_r are the mass, damping, and stiffness matrices of the track, respectively. y_r, $\dot{y}_r$ and $\ddot{y}_r$ are the displacement, velocity and acceleration responses of the track, respectively. F_{rv} is the external force excited on the track. N_r is an $n\times1$ vector, which are zeros except at the DOFs where F_{rv} is excited. n is the total DOFs of the track. $N_r=[0\ 0\ldots\ N_{ri}\ \ldots\ 0]^T$, where N_{ri} is the shape functions in the global coordinates evaluated for the ith element supporting the moving vehicle with $(i\text{-}1)\times l \le x(t) \le i\times l$. $x(t)$ is the location of the moving vehicle in the global coordinate, and l is the length of the finite element (as shown in Fig. 1). N_{ri} is obtained from functions

$$N_{ri}=\begin{Bmatrix} 1-3\left(\dfrac{x(t)-(i-1)l}{l}\right)^2+2\left(\dfrac{x(t)-(i-1)l}{l}\right)^3 \\ \left(x(t)-(i-1)l\right)\left(\dfrac{x(t)-(i-1)l}{l}-1\right)^2 \\ 3\left(\dfrac{x(t)-(i-1)l}{l}\right)^2-2\left(\dfrac{x(t)-(i-1)l}{l}\right)^3 \\ \left(x(t)-(i-1)l\right)\left(\dfrac{x(t)-(i-1)l}{l}-1\right)^2-\dfrac{\left(x(t)-(i-1)l\right)^2}{l} \end{Bmatrix} \tag{2}$$

In Eq. (1), C_r is the damping matrix. The classical Rayleigh damping matrix is adopted in this paper. The damping matrix is expressed as a linear combination of the track mass matrix M_r and the track stiffness matrix K_r, which is written as

$$[C_r]=\alpha[M_r]+\beta[K_r] \tag{3}$$

where

$$\alpha=4\pi\frac{\zeta_1 f_1 f_2^2-\zeta_2 f_1^2 f_2}{f_2^2-f_1^2},\quad \beta=\frac{1}{\pi}\frac{\zeta_2 f_2-\zeta_1 f_1}{f_2^2-f_1^2} \tag{4}$$

where f_1 and f_2 are the first and second order frequencies, respectively. ξ_1 and ξ_2 are the first and second order damping ratios of the track, respectively.

2.2 Dynamic responses analysis of the three-parameter vehicle

Vehicles running on the track are connected to the track via contact points. The vehicle-track interaction forces acting on the track F_{rv} and the interaction forces acting on the vehicles F_{vr} are actually action and reaction forces excited at the contact points. In the finite element analysis, these interaction forces may not be imposed right on a specific node. Therefore, the interaction forces need to be transformed into equivalent nodal forces.

The three-parameter vehicle consisting of a mass, spring, and damper is modeled with a single DOF, as shown in Fig. 1. The dynamic equation of the vehicle is written as

$$m_v\ddot{y}_v + c_v\dot{y}_v + k_v y_v = -F_{vr} + F_g \tag{5}$$

where m_v, c_v, and k_v are the mass, damping, and stiffness for the vehicle, respectively. y_v, $\dot{y}_v$ and $\ddot{y}_v$ are the displacement, velocity and acceleration vectors of the vehicle body, respectively. F_{vr} and F_g are the vehicle-track interaction force for the vehicle and the gravity force, respectively.

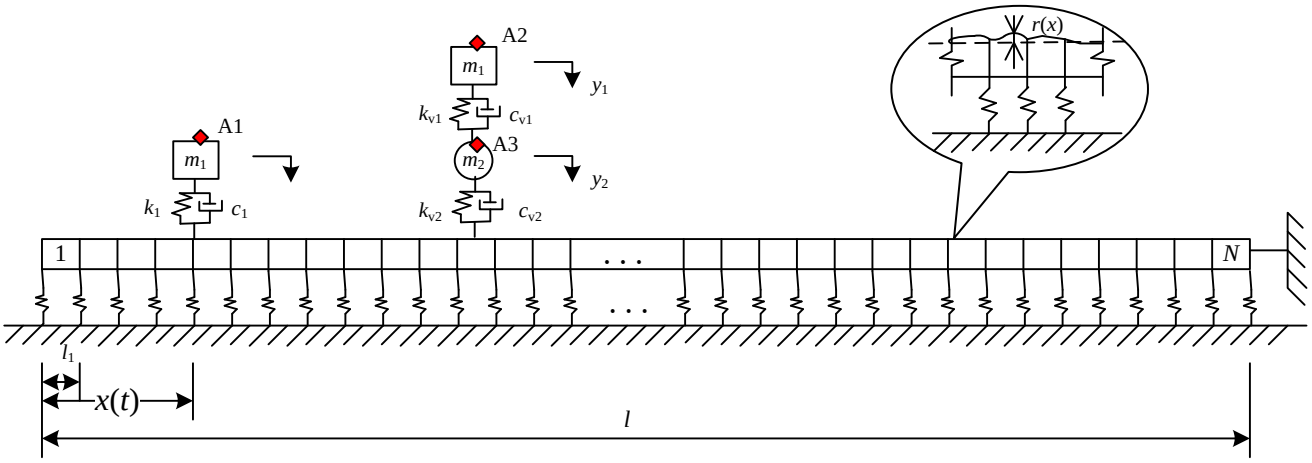

Fig. 1 The *N*-span track with different vehicle models (A1-A3:measurement points; 1 ,…, *N*: number of element)

The vehicle-track interaction force F_{vr} is expressed as

$$\begin{aligned} F_{vr} &= m_v g + c_v\left(\dot{y}_v - \dot{y}\left(x(t)\right)\right) + k_v\left(y_v - y\left(x(t)\right) - r\left(x(t)\right)\right) \\ &= m_v g - m_v \ddot{y}_v \end{aligned} \tag{6}$$

where g is the acceleration of gravity. $y(x(t))$ represents the deflection of the contact point of the deck at $x(t)$. $r(x(t))$ is the road surface roughness at $x(t)$.

The vehicle is assumed to be contacted with the track permanently and no jumps occur between the vehicle's wheels and the track. Combining Eqs. (1) and (5), the equation of motion of the vehicle-track coupling system is written as

$$\begin{bmatrix} M_r & N_r m_v \\ 0 & m_v \end{bmatrix}\begin{Bmatrix} \ddot{y}_r \\ \ddot{y}_v \end{Bmatrix} + \begin{bmatrix} C_r & 0 \\ -N_r^T c_v & c_v \end{bmatrix}\begin{Bmatrix} \dot{y}_r \\ \dot{y}_v \end{Bmatrix} + \begin{bmatrix} K_r & 0 \\ -N_r^T k_v & k_v \end{bmatrix}\begin{Bmatrix} y_r \\ y_v \end{Bmatrix} = \begin{Bmatrix} N_r m_v g \\ k_v r\left(x(t)\right) \end{Bmatrix} \tag{7}$$

Eq. (7) can be solved by the Newmark integration method (Lei and Noda 2002).

2.3 Model for the five-parameter vehicle

The five-parameter vehicle model with two DOFs (as shown in Fig. 1) comprises five components: a body mass m_{v1}, bogie mass m_{v2}, a suspension damper c_v, a suspension spring k_{v1} and another spring k_{v2} used to represent the stiffness of the tire. The dynamic equation of the vehicle is written as

$$\begin{cases} m_{v1}\ddot{y}_{v1} + c_v(\dot{y}_{v1} - \dot{y}_{v2}) + k_{v1}(y_{v1} - y_{v2}) = 0 \\ m_{v2}\ddot{y}_{v2} + c_v(\dot{y}_{v2} - \dot{y}_1) + k_{v1}(y_{v2} - y_{v1}) \\ +k_{v2}(y_{v2} - y(x(t)) - r(x(t))) = 0 \end{cases} \tag{8}$$

where y_{v1} $\dot{y}_{v1}$ and $\ddot{y}_{v1}$ are the displacement, velocity and acceleration vectors of the body of the vehicle, respectively. Similarly, y_{v2}, $\dot{y}_{v2}$ and $\ddot{y}_{v2}$ are the vertical displacement, velocity and acceleration vectors of the bogie of the vehicle, respectively. The interaction force F_{vr} between the track and the vehicle is expressed as (Bu *et al*. 2006)

$$\begin{aligned} P_{vr} &= (m_{v1} + m_{v2})g + k_{v2}(y_2 - y(x(t)) - r(x(t))) \\ &= (m_{v1} + m_{v2})g - m_{v1}\ddot{y}_1 - m_{v2}\ddot{y}_2 \end{aligned} \tag{9}$$

Combining Eqs. (1) and (9), the equation of motion of the vehicle-track system is written as

$$\begin{bmatrix} M_r & N_r m_{v1} & N_r m_{v2} \\ 0 & m_{v1} & 0 \\ 0 & 0 & m_{v2} \end{bmatrix}\begin{Bmatrix} \ddot{y}_r \\ \ddot{y}_{v1} \\ \ddot{y}_{v2} \end{Bmatrix} + \begin{bmatrix} C_r & 0 & 0 \\ 0 & c_v & -c_{v1} \\ -N_r^T c_{v2} & c_{v1} & c_{v1} + c_{v2} \end{bmatrix}\begin{Bmatrix} \dot{y}_r \\ \dot{y}_{v1} \\ \dot{y}_{v2} \end{Bmatrix} + \begin{bmatrix} K_r & 0 & 0 \\ 0 & k_{v1} & -k_{v1} \\ -N_r^T k_{v2} & -k_{v1} & k_{v1} + k_{v2} \end{bmatrix}\begin{Bmatrix} y_r \\ y_{v1} \\ y_{v2} \end{Bmatrix} = \begin{Bmatrix} N_r(m_{v1} + m_{v2})g \\ 0 \\ k_{v2} r\left(x(t)\right) \end{Bmatrix} \tag{10}$$

Identically, Eq. (10) is also available with the Newmark integration method.

Actually, the vibration equations of the vehicle and track coupling system for the three-parameter vehicle model and the five-parameter vehicle model (Eqs. (7) and (10)) can be rewritten in a generalized form as

$$\begin{bmatrix} M_r & N_r M_v \\ 0 & M_v \end{bmatrix}\begin{Bmatrix} \ddot{y}_r \\ \ddot{y}_v \end{Bmatrix} + \begin{bmatrix} C_r & 0 \\ -N_r^T C_v & C_v \end{bmatrix}\begin{Bmatrix} \dot{y}_r \\ \dot{y}_v \end{Bmatrix} + \begin{bmatrix} K_r & 0 \\ -N_r^T K_v & K_v \end{bmatrix}\begin{Bmatrix} y_r \\ y_v \end{Bmatrix} = \begin{Bmatrix} N_r m_v g \\ K_v r\left(x(t)\right) \end{Bmatrix} \tag{11}$$

where M_v, K_v and C_v are the mass, stiffness and damping matrix of the vehicles. For a vehicle model with x DOFs, M_v=diag(m_{v1}, m_{v2},…, m_{vx}), K_v=diag(k_{v1}, k_{v2},…, k_{vx}), C_v=diag(c_{v1}, c_{v2},…, c_{vx}). It should be noted that Eq. (11) can be used for complicated vehicle models with enormous DOFs and Eqs. (7) and (10) are just its particular cases.

3. Numerical simulation of the random irregularity of track vertical profile

The track irregularity is a non-negligible excitation of

the vehicle-track coupling system. For the vehicle-track coupling system, there is an assumption that the vehicle never detach from the track and the only connection between the vehicle and track is the track irregularity.

The irregularity of the track vertical profile is regarded as the stationary ergodic Gaussian random processes except for the area with turnout, road crossing and the rail line with track deterioration. In this paper, considering a stationary stochastic process $r(t)$ with the expectation of zero and the power density function of $\Phi(\omega)$, the sample function of the stochastic process $r(t)$ is simulated by the trigonometry series shown as (Lei *et al*. 2002)

$$r(t)=\sum_{\xi=1}^{R} a_{\xi}\sin\left(\omega_{\xi}t+\phi_{\xi}\right) \tag{12}$$

where a_{ξ} is a Gaussian random variable with the expectation of zero and the variance of σ_{ξ}, and is independent for ξ=1, 2, … , R (R is large enough). ϕ_{ξ} is a random variable distributed uniformly in 0~2π, and is independent for ξ as well. A_{ξ} and ϕ_{ξ} are irrelevant to each other, which are calculated by Monte Carlo method.

In order to obtain the variance σ_{ξ}, a frequency band $\Delta\omega$ is defined as

$$\Delta\omega=\left(\omega_u-\omega_l\right)/R \tag{13}$$

where ω_l and ω_u are the lower and upper boundary frequencies in the frequency domain of power spectral density function $\Phi(\omega)$.

The intermediate variable ω_{ξ} is defined as

$$\omega_{\xi}=\omega_l+\left(\xi-\frac{1}{2}\right)\Delta\omega \tag{14}$$

σ_{ξ} is expressed as

$$\sigma_{\xi}^2=4\Phi\left(\omega_{\xi}\right)\Delta\omega \tag{15}$$

In the above equations, the effective power spectral density $\Phi(\omega)$ is

$$\Phi\left(\omega\right)=\begin{cases}\Phi\left(\omega_{\xi}\right) & \omega_l\le\omega_{\xi}\le\omega_u\\ 0 & else\end{cases} \tag{16}$$

The power spectral density $\Phi(\omega)$ of the track for the line grades of one to six from American Railway Standard is used as input excitation (Lei *et al*. 2002), which has

$$\Phi\left(\omega\right)=\frac{\kappa A_{\xi}\omega_c^2}{\left(\omega^2+\omega_c^2\right)\omega^2} \tag{17}$$

Table 1 Coefficients for A_{ξ} and ω_c

Line grade	A_{ξ}(cm^2rad/m)	ω_c(rad/m)
1	1.2107	0.8245
2	1.0181	0.8245
3	0.6816	0.8245
4	0.5376	0.8245
5	0.2095	0.8245
6	0.0339	0.8245

where A_{ξ} and ω_c are coefficients associated with line grade, as shown in Table 1, and κ is a constant, which is set to 0.25 generally.

4. Dynamic response sensitivity with respect to the damage index

4.1 Three-parameter vehicle model

For the three-parameter vehicle model, differentiating both sides of Eq. (8) with respect to the elemental damage index of the jth element gives

$$\begin{aligned}&\frac{\partial}{\partial\gamma^j}\left\{\begin{bmatrix}M_r & N_rm_v\\ 0 & m_v\end{bmatrix}\begin{Bmatrix}\ddot{y}_r\\ \ddot{y}_v\end{Bmatrix}\right\}+\frac{\partial}{\partial\gamma^j}\left\{\begin{bmatrix}C_r & 0\\ -N_r^Tc_v & c_v\end{bmatrix}\begin{Bmatrix}\dot{y}_r\\ \dot{y}_v\end{Bmatrix}\right\}+\\ &\frac{\partial}{\partial\gamma^j}\left\{\begin{bmatrix}K_r & 0\\ -N_r^TK_v & k_v\end{bmatrix}\begin{Bmatrix}y_r\\ y_v\end{Bmatrix}\right\}+\begin{bmatrix}M_r & N_rm_v\\ 0 & m_v\end{bmatrix}\begin{Bmatrix}\frac{\partial\ddot{y}_r}{\partial\gamma^j}\\ \frac{\partial\ddot{y}_v}{\partial\gamma^j}\end{Bmatrix}+\\ &\begin{bmatrix}C_r & 0\\ -N_r^Tc_v & c_v\end{bmatrix}\begin{Bmatrix}\frac{\partial\dot{y}_r}{\partial\gamma^j}\\ \frac{\partial\dot{y}_v}{\partial\gamma^j}\end{Bmatrix}+\begin{bmatrix}K_r & 0\\ -N_r^Tm_v & m_v\end{bmatrix}\begin{Bmatrix}\frac{\partial y_r}{\partial\gamma^j}\\ \frac{\partial y_v}{\partial\gamma^j}\end{Bmatrix}=\frac{\partial}{\partial\gamma^j}\begin{Bmatrix}N_rm_vg\\ k_vr\left(x(t)\right)\end{Bmatrix}\end{aligned} \tag{18}$$

It is noted from Eqs. (1), (3) and (5) that K_r and C_r are relevant to γ^j, and m_v, c_v, k_v, N_r and $r(x(t))$ are irrelevant to γ^j . In consequence, γ^j is related to K_r as

$$\frac{\partial C_r}{\partial\gamma^j}=\beta\frac{\partial K_r}{\partial\gamma^j} \tag{18}$$

Eq. (17) is simplified as

$$\begin{aligned}&\begin{bmatrix}M_r & N_rm_v\\ 0 & m_v\end{bmatrix}\begin{Bmatrix}\frac{\partial\ddot{y}_r}{\partial\gamma^j}\\ \frac{\partial\ddot{y}_v}{\partial\gamma^j}\end{Bmatrix}+\begin{bmatrix}C_r & 0\\ -N_r^Tc_v & c_v\end{bmatrix}\begin{Bmatrix}\frac{\partial\dot{y}_r}{\partial\gamma^j}\\ \frac{\partial\dot{y}_v}{\partial\gamma^j}\end{Bmatrix}\\ &+\begin{bmatrix}K_r & 0\\ -N_r^Tk_v & k_v\end{bmatrix}\begin{Bmatrix}\frac{\partial y_r}{\partial\gamma^j}\\ \frac{\partial y_v}{\partial\gamma^j}\end{Bmatrix}=\begin{Bmatrix}-\frac{\partial K_r}{\partial\left(\gamma^j\right)}y_r-\beta\frac{\partial K_r}{\partial\gamma^j}\dot{y}_r\\ 0\end{Bmatrix}\end{aligned} \tag{20}$$

It is observed from the above equation that the displacement response y_r and velocity response $\dot{y}_r$, obtained from Eq. (7), is the input data for Eq. (20). The response sensitivities of the track DOFs and vehicle DOFs can be calculated from Eq. (20) by the Newmark integration method.

4.2 Five-parameter vehicle model

Similarly, for the five-parameter vehicle model, differentiating both sides of Eq. (10) with respect to the damage index γ^j, of the jth element leads to

$$\begin{aligned}&\begin{bmatrix}M_r & 0 & 0\\ 0 & m_{v1} & 0\\ 0 & 0 & m_{v2}\end{bmatrix}\begin{Bmatrix}\frac{\partial\ddot{Z}_r}{\partial\gamma^j}\\ \frac{\partial\ddot{Z}_{v1}}{\partial\gamma^j}\\ \frac{\partial\ddot{Z}_{v2}}{\partial\gamma^j}\end{Bmatrix}+\begin{bmatrix}C_r & 0 & 0\\ 0 & c_v & -c_v\\ 0 & c_v & c_v\end{bmatrix}\begin{Bmatrix}\frac{\partial\dot{Z}_r}{\partial\gamma^j}\\ \frac{\partial\dot{Z}_{v1}}{\partial\gamma^j}\\ \frac{\partial\dot{Z}_{v2}}{\partial\gamma^j}\end{Bmatrix}+\begin{bmatrix}K_r & 0 & 0\\ 0 & k_{v1} & -k_{v1}\\ 0 & -k_{v1} & k_{v1}+k_{v2}\end{bmatrix}\begin{Bmatrix}\frac{\partial Z_r}{\partial\gamma^j}\\ \frac{\partial Z_{v1}}{\partial\gamma^j}\\ \frac{\partial Z_{v2}}{\partial\gamma^j}\end{Bmatrix}\\ &=\begin{Bmatrix}-\frac{\partial K_r}{\partial\gamma^j}Z_r-\beta\frac{\partial K_r}{\partial\gamma^j}\dot{Z}_r\\ 0\\ 0\end{Bmatrix}-\begin{Bmatrix}N_rm_{v1}\frac{\partial\ddot{Z}_{v1}}{\partial\gamma^j}+N_rm_{v2}\frac{\partial\ddot{Z}_{v2}}{\partial\gamma^j}\\ 0\\ -N_r^Tk_{v2}\frac{\partial Z_r}{\partial\gamma^j}\end{Bmatrix}\end{aligned} \tag{21}$$

The response sensitivities of the track DOFs and vehicle DOFs are calculated from Eq. (21) by the Newmark method. The right hand side of Eq. (21) is regarded as the equivalent force, which can be calculated from Eq. (10). In this paper, only the response sensitivities of the vehicle DOFs are used to construct the sensitivity matrix.

4.3 Sensitivity of response with respect to vehicular parameters

In this part, Eq. (11) is used to illustrate the influence of vehicle parameters to the identification of the track damages. Differentiating both sides of Eq. (7) with respect to the mass of the rigid body of the vehicle m_v, stiffness k_v, damping c_v, respectively.

$$\begin{bmatrix} M_r & N_r m_v \\ 0 & m_v \end{bmatrix} \begin{Bmatrix} \dfrac{\partial \ddot{y}_r}{\partial m_v} \\ \dfrac{\partial \ddot{y}_v}{\partial m_v} \end{Bmatrix} + \begin{bmatrix} C_r & 0 \\ -N_r^T c_v & c_v \end{bmatrix} \begin{Bmatrix} \dfrac{\partial \dot{y}_r}{\partial m_v} \\ \dfrac{\partial \dot{y}_v}{\partial m_v} \end{Bmatrix} + \begin{bmatrix} K_r & 0 \\ -N_r^T k_v & k_v \end{bmatrix} \begin{Bmatrix} \dfrac{\partial y_r}{\partial m_v} \\ \dfrac{\partial y_v}{\partial m_v} \end{Bmatrix} = \begin{Bmatrix} N_r g \\ 0 \end{Bmatrix} \tag{22}$$

$$\begin{bmatrix} M_r & N_r m_v \\ 0 & m_v \end{bmatrix} \begin{Bmatrix} \dfrac{\partial \ddot{y}_r}{\partial k_v} \\ \dfrac{\partial \ddot{y}_v}{\partial k_v} \end{Bmatrix} + \begin{bmatrix} C_r & 0 \\ -N_r^T c_v & c_v \end{bmatrix} \begin{Bmatrix} \dfrac{\partial \dot{y}_r}{\partial k_v} \\ \dfrac{\partial \dot{y}_v}{\partial k_v} \end{Bmatrix} + \begin{bmatrix} K_r & 0 \\ -N_r^T k_v & k_v \end{bmatrix} \begin{Bmatrix} \dfrac{\partial y_r}{\partial k_v} \\ \dfrac{\partial y_v}{\partial k_v} \end{Bmatrix} = \begin{Bmatrix} 0 \\ r(x(t)) \end{Bmatrix} \tag{23}$$

$$\begin{bmatrix} M_r & N_r m_v \\ 0 & m_v \end{bmatrix} \begin{Bmatrix} \dfrac{\partial \ddot{y}_r}{\partial c_v} \\ \dfrac{\partial \ddot{y}_v}{\partial c_v} \end{Bmatrix} + \begin{bmatrix} C_r & 0 \\ -N_r^T c_v & c_v \end{bmatrix} \begin{Bmatrix} \dfrac{\partial \dot{y}_r}{\partial c_v} \\ \dfrac{\partial \dot{y}_v}{\partial c_v} \end{Bmatrix} + \begin{bmatrix} K_r & 0 \\ -N_r^T k_v & k_v \end{bmatrix} \begin{Bmatrix} \dfrac{\partial y_r}{\partial c_v} \\ \dfrac{\partial y_v}{\partial c_v} \end{Bmatrix} = \begin{Bmatrix} 0 \\ 0 \end{Bmatrix} \tag{24}$$

Then the response sensitivity with respect to the parameters of the vehicle can be obtained from Eqs. (22)-(24).

5. Identification of the local damages from measured dynamic responses

The damage identification is often conducted based on a sensitivity-based model updating process. Many elemental physical parameters, such as stiffness reduction, vehicle parameters and so on, can be used as damage indices. Except for some special cases, it is usually assumed that damage does not change the mass but the stiffness of the structure. In this paper, only the stiffness reduction of the track has been considered. Name the undamaged stiffness and the associated damage index of the jth element in the associated state are γ^j and $(EI)_U{}^j$, its stiffness in the damaged state can be written as

$$(EI)_D{}^j = (EI)_U{}^j (1-\gamma^j) \quad (0 \le \gamma^j \le 1) \tag{25}$$

It is assumed that a track with N elements has the damage index vector A_γ. A_γ encloses the whole damage indices of the track elements ($A_\gamma=\{\gamma^1, \gamma^2, \dots, \gamma^N\}^T$). The damage identification is conducted to identify damage index vector A_γ by reproducing the measured responses R^m with the calculated responses R^c through an iterative process. R^m is expressed as

$$\{R^m\} = [Q]\{R^c\} \tag{26}$$

where $[Q]$ is a selection matrix, which is sparse and ones only at the DOFs corresponding to the measured points. The primary task is to minimize the error between the calculated responses and measured ones as

$$\delta R = \{R^m\} - [Q]\{R^c\} \tag{27}$$

Using the common penalty function method (Hansen *et al*. 2008), the sensitivity equation for damage identification is expressed as

$$[S_\gamma] \times \{\delta A_\gamma\} = \{\delta R\} \tag{28}$$

$\{\delta A_\gamma\}$ is the perturbation in the damage index vector, $[S_\gamma]$ is a time varying response sensitivity matrix, which contains the partial derivatives of the dynamic response with respect to the damage index. Construct the time-varying sensitivity matrix as

$$S_v^\gamma = \begin{bmatrix} \dfrac{\partial \ddot{y}_v(t_1)}{\partial \gamma^1} & \dfrac{\partial \ddot{y}_v(t_1)}{\partial \gamma^2} & \cdots & \dfrac{\partial \ddot{y}_v(t_1)}{\partial \gamma^N} \\ \dfrac{\partial \ddot{y}_v(t_2)}{\partial \gamma^1} & \dfrac{\partial \ddot{y}_v(t_2)}{\partial \gamma^2} & \cdots & \dfrac{\partial R_2^c(t_2)}{\partial \gamma^N} \\ \vdots & \vdots & \cdots & \vdots \\ \dfrac{\partial \ddot{y}_v(t_i)}{\partial \gamma^1} & \dfrac{\partial \ddot{y}_v(t_i)}{\partial \gamma^2} & \cdots & \dfrac{\partial \ddot{y}_v(t_i)}{\partial \gamma^N} \\ \vdots & \vdots & \cdots & \vdots \\ \dfrac{\partial \ddot{y}_v(t_q)}{\partial \gamma^1} & \dfrac{\partial \ddot{y}_v(t_q)}{\partial \gamma^2} & \cdots & \dfrac{\partial \ddot{y}_v(t_q)}{\partial \gamma^N} \end{bmatrix}_{q \times N} \tag{29}$$

where N_M is the total number of time steps. Eq. (27) can be solved by least-squares method (Liu *et al*. 2009) as

$$\{\delta A_\gamma\} = \left([S_\gamma]^T [S_\gamma]\right)^{-1} [S_\gamma]^T \{\delta R\} \tag{30}$$

Since N_M is often larger than the number of unknown parameters, Eq. (29) is an ill-conditioned system of equations with unstable solutions. In order to provide bounds to the sensitivity equation, the damped least-squares method (Jiang *et al*. 2004) and singular value decomposition technique are used in the pseudo-inverse calculation. Eq. (29) is then rewritten as

$$\{\delta A_\gamma\} = \left([S_\gamma]^T [S_\gamma] + \lambda I\right)^{-1} [S_\gamma]^T \{\delta R\} \tag{31}$$

where λ is the non-negative damping coefficient to determine the participation of least-squares error in the

solutions. The solution of Eq. (30) is achieved by minimizing the function

$$J\left(\left\{\delta A_\gamma\right\},\lambda\right)=\left\|\left[S_\gamma\right]\delta A_\gamma-\delta R\right\|^2+\lambda\left\|\delta A_\gamma\right\|^2 \tag{32}$$

where the second term ($\lambda\left\|\delta A_\gamma\right\|^2$) gives bounds to the solution. When the parameter λ approaches zero, the estimated vector $\{\delta A_\gamma\}$ approaches the solution obtained from the least-squares method.

Many methods have been developed to get the optimal regularization parameter λ. In this paper, the well-known L-curve method (Zhan *et al*. 2011) is used to determine λ.

Once the increment in the elemental flexural rigidity vector $\{\delta A_\gamma\}$ is obtained from Eq. (30), the updated element flexural rigidity is expressed as

$$\left\{A_\gamma\right\}=\left\{A_\gamma\right\}_0+\left\{\delta A_\gamma\right\} \tag{33}$$

The following convergence criterion is used as

$$\left\|\frac{\left\{\left(A_\gamma\right)_{k+1}\right\}-\left\{\left(A_\gamma\right)_k\right\}}{\left\{\left(A_\gamma\right)_{k+1}\right\}}\right\|\le\varepsilon_\gamma \tag{34}$$

where $\|\cdot\|$ means the norm of a vector.

Overall, two main problems arise to conduct the above sensitivity-based damage identification process. Firstly, the structural dynamic responses are employed to construct the objective function. Secondly, the responses sensitivity matrices used to provide a rapid searching direction.

6. Numerical example

A numerical vehicle-track coupling system is studied to illustrate the feasibility and efficiency of the proposed damage identification method. As shown in Fig. 1, the track system is modeled as a beam which is supported by discrete points with the span of l=100 m. The discrete point supported beam is divided into 100 elements (N=100) with each 1 m in length. The beam has 101 nodes and 300 DOFs in total. The material constants of the beam elements are chosen as: Young's modulus E=33 GPa, cross sectional area A=600 mm×1000 mm, volume density ρ=3500 kg/m^3, and Poisson's ratio μ=0.15. Two commonly used vehicle models, three-parameter vehicle model and five-parameter vehicle model, are used in this paper to compare their damage identification results. The coefficients of the three-parameter vehicle model are: m_v=2500 kg, c_v=1000 Ns/m and k_v=6.0×10^5 N/m. The coefficients of the five-parameter vehicle model are: m_{v1}=3600 kg, m_{v2}=250 kg, c_v=1000 Ns/m, k_{v1}=6.0×10^5 N/m and k_{v2}=8.5×10^5 N/m. The speed of the vehicle v is set to 20 m/s and the time step in the response calculation is 0.002s. The total number of time steps N_M is 2501. The lower and upper boundary frequencies ω_l=(0.04π) rad/s and ω_u=(4π) rad/s. N_T is set to 2500. The track random irregularity chosen in this paper is shown in Fig. 2.

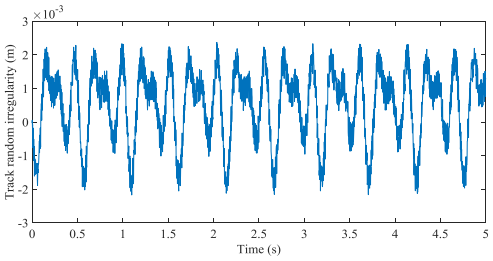

Fig. 2 The track random irregularity adopted in this paper

For the three-parameter vehicle model, the acceleration response of the measured point A1 (as shown in Fig. 1) is used for the damage identification. For the five-parameter vehicle model, two acceleration measured points A2-A3, located at the body and the bogie of the vehicle respectively, are used for damage identification.

Since measurement noise is inevitable and a certain level of noise may cause inaccurate identification results in practical tests, investigation on the effects of measurement noises of the vehicle responses is significant.

To estimate the damage identification results on a certain degree of measurement noise, noise-polluted measurements are simulated by adding an associated noise vector with the noise-free acceleration vector.

The measurement noise of the responses of the vehicle is assumed to be normally randomly distributed (Lu *et al*. 2007). The polluted response is thus expressed as

$$y_c^{\,p}=y_c+e_pN_0\sigma\left(y_c\right) \tag{35}$$

where $y_c^{\,p}$ and y_c are the polluted response and the calculated counterpart, respectively. e_p is the ratio of the noise amplitude to the response amplitude ($0\le e_p\le 1$). N_0 is the standard normal distribution vector. $\sigma(y_c)$ is the standard deviation of the calculated response, which indicates the deviation of the response to its mean value. Two different levels of noise (5% and 10%) were considered in the present study.

In this part, the acceleration measurement point A1 is used to identify the damage of the track. The stiffness of 3nd, 22th and 81th element are assumed to be reduced by 15%, 30% and 20%, respectively, namely γ^3, γ^{22} and γ^{81} are 0.15, 0.3 and 0.2. The proposed method is utilized to identify the location and severity of the assumed stiffness reductions.

The detailed procedures of the damage identification of the track by the proposed method are described as follows:

1) Calculate the constants to be used in later work.

a. Assemble the mass matrix $\begin{bmatrix}M_r & \\ & m_v\end{bmatrix}$, stiffness matrix $\begin{bmatrix}K_r & \\ & k_v\end{bmatrix}$ and damping matrix $\begin{bmatrix}C_r & \\ & c_v\end{bmatrix}$ of the vehicle-track coupling system independently.

b. Calculate the track surface roughness $r(x(t))$ from Eq. (11) and the shape function N_r from Eq. (2).

c. Compute the equivalent force vector $\begin{bmatrix}N_r m_v g \\ k_v r\left(x(t)\right)\end{bmatrix}$.

2) Calculate the dynamic responses of the vehicle-track coupling system from Eq. (7) using the Newmark method in damaged and undamaged states, namely ($\begin{bmatrix} y_r \\ y_v \end{bmatrix}^m$, $\begin{bmatrix} \dot{y}_r \\ \dot{y}_v \end{bmatrix}^m$, $\begin{bmatrix} \ddot{y}_r \\ \ddot{y}_v \end{bmatrix}^m$) and ($\begin{bmatrix} y_r \\ y_v \end{bmatrix}^c$, $\begin{bmatrix} \dot{y}_r \\ \dot{y}_v \end{bmatrix}^c$, $\begin{bmatrix} \ddot{y}_r \\ \ddot{y}_v \end{bmatrix}^c$).

3) Gain the acceleration derivative $\frac{\partial \ddot{y}_v}{\partial \gamma^j}$ from Eq. (12) by Newmark method. Then construct the sensitivity matrix $[S_\gamma]$ according to Eq. (28).

4) Construct the objective function $\delta R = \ddot{y}_v^{\,c} - \ddot{y}_v^{\,m}$ using the acceleration responses of the vehicle $\ddot{y}_v^{\,c}$ and $\ddot{y}_v^{\,m}$.

5) Calculate the increment in the damage index vector $[\delta A_\gamma]$ from Eq. (29). Identify the damage indices from Eq. (30).

The accuracy of the proposed damage identification method is first studied without noise. The damage identification of the track is performed following the above steps, with the identified damage indices of all elements listed in Fig. 3. It is obvious that the damage indices of Elements 3, 22 and 81 are about 15%, 30% and 20% respectively while those of the other damage indices are near zeros, which agrees with the assumed damage location and severity. The exact identification values of the indices of Elements 3, 22 and 81 are compared with the assumed ones in Table 2.

The damage indices of Elements 3, 22 and 81 are 14.608%, 29.748% and 19.954%, respectively. The identified errors are 0.392%, 0.252% and 0.046% at Elements 3, 22 and 81, which are much less than 1%. Therefore, the vehicle acceleration measurement response of A1 can be used to identify the location and severity of the local damage correctly.

Table 2 Identified results using acceleration responses of A1

Element No.	RDV* (%)	DIV* (%)	RE* (%)
3	15	14.608	0.392
22	30	29.748	0.252
81	20	19.954	0.046

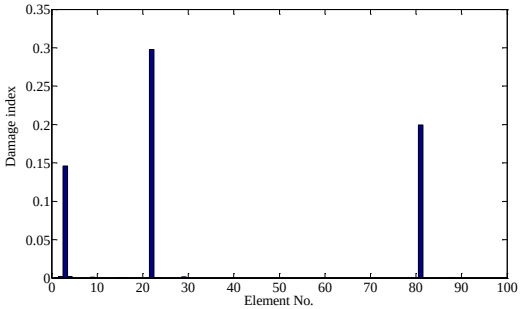

Fig. 3 Damage indices identification using acceleration responses of A1

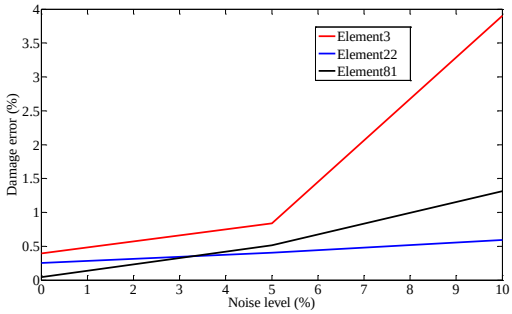

Fig. 4 Damage identification using acceleration responses of A1 under different noise levels

Then the effects of the measurement noise on the proposed damage identification method are studied. Identically, the bending rigidities of Elements 3, 22 and 81 are assumed to be reduced by 10%, 30% and 20% respectively, while those of the other elements remain unchanged. Using the proposed method, the damage indices of all track elements under different noise levels are identified. For clarity, the identified damage errors of the selected elements are listed in Fig. 4.

It is noted that the identified damage errors of all the selected elements are less than 0.5% in zero noise level, which again verifies that the proposed damage identification method is very accurate when no measurement noise is considered. Then, the identified damage errors rise with the increase of the noise level. Finally, even the noise level reaches 10%, the damage errors of all the selected elements are still less than 5%, which is acceptable in practical engineering. Actually, the measurement noise seldom reaches 10% in practical engineering. Therefore, the proposed method is accurate to identify the local damages of vehicle-track system.

Since too much noise influences the accuracy of the damage identification results, some measures should also be taken to restrict the measurement noise to an appropriate level. In this part, the acceleration measurement points A2 and A3, located at the body and the bogie of the vehicle, are used to identify the local damages of the track. Similarly, the stiffness of track Elements 3, 22 and 81 are assumed to be reduced by 15%, 30% and 20% respectively. That is, γ^3=0.15, γ^{22}=0.3 and γ^{81}=0.2. The damage identification of the five-parameter model is conducted with a similar process to the three-parameter model. The measured acceleration responses of A2 and A3 are used in the proposed damage identification method, with the identified damage indices drawn in Figs. 5 and 6 respectively.

It is noted that both Figs. 5 and 6 reveal obvious stiffness reductions in Elements 3, 22 and 81, which agrees with the assumed damage location well. However, some small stiffness reductions of other track elements are identified in Fig. 5 while nearly no corresponding damage is identified in Fig. 6. Therefore, both the measured vehicle acceleration responses of A2 and A3 are effective to be used in the damage location of vehicle-track system, yet those of A3 reveal superiority in terms of accuracy.

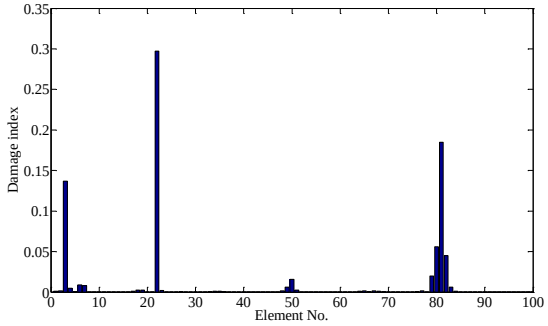

Fig. 5 Damage indices identification using acceleration responses of A2

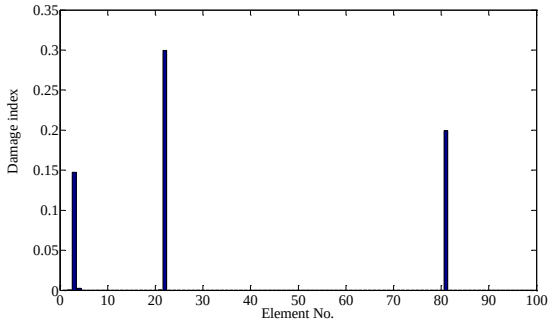

Fig. 6 Damage indices identification using acceleration responses of A3

Table 3 Identified results using acceleration responses of A2 and A3

Element No.	RDV (%)	Point No.			
		A2		A3	
		DIV (%)	RE (%)	DIV (%)	RE (%)
3	15	14.405	1.310	14.849	0.151
22	30	29.734	0.268	29.953	0.047
81	20	19.954	1.512	19.960	0.040

To estimate the accuracy of the identification results using the measured responses of A2 and A3, the exact damage indices of Elements 3, 22 and 81 are listed in Table 3. Using the measured acceleration response of A2 in the proposed damage identification method, the relative errors of the identified damage indices of Elements 3, 22 and 81 are 1.310%, 0.268% and 1.512%. But when the measured acceleration response of A3 is applied, the corresponding relative errors are 0.151%, 0.047% and 0.040%, which are much smaller than those of A2. It again verifies that the measured acceleration responses of A3 are more accurate than those of A2 in the precision of damage identification.

To compare the efficiency of the proposed damage identification method using different measured points (A2 and A3), the computation time and the relative error of damage indices are recorded step by step. The convergence of the damage identification process using the acceleration responses of A2 and A3 are illustrated in Fig. 7. It is evident that the curve of A3 converges much faster than that of A2. For example, it takes about 40 minutes for the relative error of A3 to reach 0.1%, about half of that of A2. As a conclusion, it is much more efficient to use the measured acceleration responses of A3 in the proposed damage identification method.

The damage indices of all the track elements are identified under different noise levels. For clarity, Fig. 9 compares the damage indices without noise and 10% noise using acceleration dynamic responses of A2. It is seen that the proposed method is accurate to identify the assumed damages under different noise levels, while that without noise is slightly more accurate.

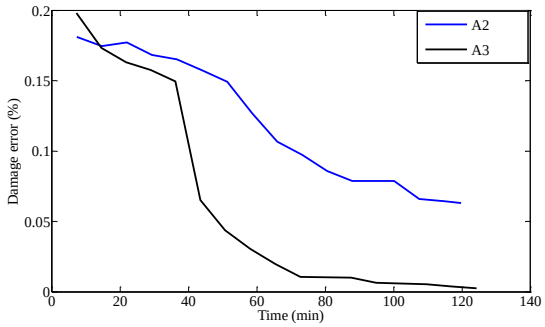

Fig. 7 Convergence of damage identification of Element 81 using acceleration responses of A2 and A3

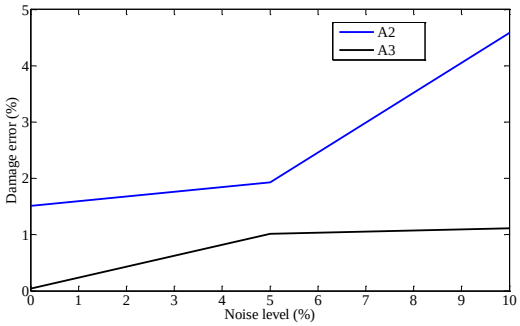

Fig. 8 Damage identification result of Element 81 under different noise levels

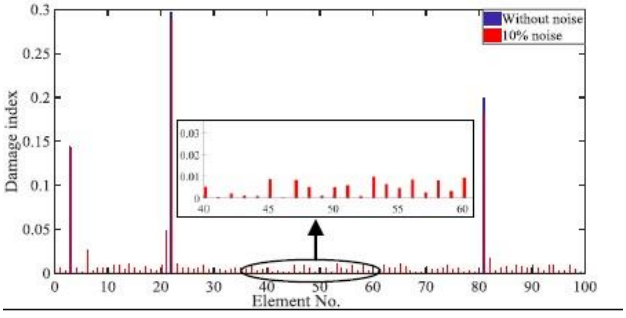

Fig. 9 Damage identification result using acceleration responses of A2 under different noise levels

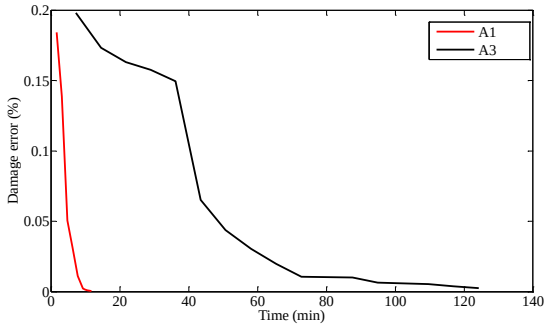

Fig. 10 The convergence of damage identification of Element 81 using acceleration responses of A1 and A3

Overall, as for the five-parameter vehicle model, the measured acceleration response of A3 is superior to that of A2 to be used in damage identification in terms of accuracy, efficiency and the effects of measurement noise. It may because that the body is not connected with the wheel directly.

Forwardly, the computational efficiency of damage identification of the two presented vehicle models (three-parameter model and five-parameter model) is compared in Fig. 10. Here the identification result of five-parameter is represented by that of A3. It is evident that the curve of A1 converges much faster than that of A3, which implies that the three-parameter model is more efficient to be used in the damage identification of vehicle-track system. This is because the vehicle-track system with five-parameter vehicle model is more complicated than that of three-parameter vehicle model. More computational resources and time are thus consumed to calculate the structural responses and response sensitivity in damage identification of the track. However, five-parameter vehicle model has been verified in many literatures (Yang *et al*. 2005, Zhang *et al*. 2016) to be advantageous to three-parameter vehicle model in dynamic analysis of the vehicle, which deserves further study in our future work.

7. Conclusions

This paper proposes a damage identification method of the vehicle-track coupling system using the vehicle responses. The responses and response sensitivities of the commonly used three-parameter vehicle model and five-parameter vehicle model are derived. The damage identification is performed based on a sensitivity-based finite element model updating process.

A numerical discrete point supported beam is used to stimulate the vehicle-track system. The accuracy and efficiency of the three-parameter model and the five-parameter model in damage identification are compared. The effects of the measurement noise on the damage identification results are also considered. The following conclusions can be made from the numerical study:

1) Both the responses of the three-parameter vehicle model and five-parameter vehicle model are feasible for the damage identification of the vehicle-track system, while the three-parameter vehicle model shows a higher efficiency.

2) The accuracy of damage identification of both the two models is influenced by the measurement noise. Some measures should be taken to restrict the noise to an appropriate level to ensure a higher precision.

3) As for the five-parameter vehicle model, it is much more efficient to employ the measured responses of the vehicle bogie for damage identification than the vehicle body.

Acknowledgments

The author would like to acknowledge the support provided by National Natural Science Foundation of China (NSFC, contract number: 51778258 and 51578260), Basic Research Program of China (2016YFC0802002), Fundamental Research Funds of the Central Universities (HUST: 2016JCTD113, 2014TS130 and 2015MS064).

References

Alvandi, A. and Cremona, C. (2006), "Assessment of vibration-based damage identification techniques", *J. Sound. Vib.*, **292**, 179-202.

Au, F.T.K., Jiang, R.J. and Cheung, Y.K. (2004), "Parameter identification of vehicles moving on continuous bridges", *J. Sound Vib.*, **269**, 91-111.

Bu, J.Q., Law, S.S., Zhu, X.Q. and Chan, S.L. (2006), "Vehicle condition surveillance on continuous bridges based on response sensitivity", *P. I. Mech. Eng. C-J. Mec.*, **132**(1), 78-86.

Chen, Y.B., Feng, M.Q. and Tan, C.A. (2009), "Bridge structural condition assessment based on vibration and traffic monitoring", *J. Eng. Mech. -ASCE*, **135**(8), 747.

Deng, L. and Cai, C.S. (2009), "Identification of parameters of vehicles moving on bridges", *Eng. Struct.*, **31**, 2474-2485.

Fan, W. and Qiao, P.Z. (2010), "Vibration-based damage identification methods: a review and comparative study", *Struct. Health Monit.*, **10**(1), 83-129.

Feng, D.M. and Feng, M.Q. (2017), "Identification of structural stiffness and excitation forces in time domain using noncontact vision-based displacement measurement", *J. Sound. Vib.*, **406**, 15-28.

Gonzalez, A., Rowley, C. and O'Brien, E.J. (2008), "A general solution to the identification of moving vehicle forces on a bridge", *Int. J. Numer. Meth. Eng.*, **75**(3), 335-354.

Guo, C. (2000), "Analysis of random vibration for vehicle and track coupling system", Ph.D. Dissertation, South West Jiaotong University, Chengdu.

He, W.Y., Ren, W.X. and Zhu, S.Y. (2017), "Damage detection of beam structures using quasi-static moving load induced displacement response", *Eng. Struct.*, **145**, 70-82.

Jiang, R.J., Au, F.T.K. and Cheung, Y.K. (2004), "Identification of vehicles moving on continuous bridges with road surface", *J. Sound Vib.*, **274**, 1045-1063.

Kong, X., Cai, C.S. and Kong, B. (2014), "Damage detection based on transmissibility of a vehicle and bridge coupled system", *J. Eng. Mech. -ASCE*, 141.

Kraft, S., Puel, G., Aubry, D. and Funfschilling, C. (2016), "Parameter identification of mult-body railway vehicle models-Application of the adjoint state approach", *Mech. Syst. Signal Pr.*, **80**, 517-532.

Kunwar, A., Jha, R., Whelan, M. and Janoyan, K. (2013), "Damage detection in an experimental bridge model using

Hilbert-Huang transform of transient vibrations", *Struct. Control Health Monit.*, **20**, 1-15.
Lei, X. and Noda, N.A. (2002), "Analyses of dynamic response of vehicle and track coupling system with random irregularity of track vertical profile", *J. Sound. Vib.*, **258**(1), 147-165.
Lu, Z.R. and Law, S.S. (2007), "Features of dynamic response sensitivity and its application in damage detection", *J. Sound Vib.*, **303**(1-2), 305-329.
Majumder, L. and Manohar, C.S. (2003), "A time-domain approach for damage detection in beam structures using vibration data with a moving oscillator as an excitation source", *J. Sound. Vib.*, **268**, 699-716.
Ni, Y.Q., Ye, X.W. and Ko, J.M. (2010), "Monitoring-based fatigue reliability assessment of steel bridges: analytical model and application", *J. Struct. Eng.-ASCE*, **163**(12), 1563-1573.
Ni, Y.Q., Ye, X.W. and Ko, J.M. (2012), "Modeling of stress spectrum using long-term monitoring data and finite mixture distributions", *J. Struct. Eng.-ASCE*, **138**(2), 175-183.
Pakrashi, V., O'Connor, A. and Basu, B. (2010), "A bridge-vehicle interaction based experimental investigation of damage evolution", *Struct. Health Monit.*, **9**(4), 285-312.
Yang, Y.B. and Lin. C.W. (2005), "Vehicle-bridge interaction dynamics and potential applications", *J. Sound Vib.*, **284**, 205-226.
Zhan, J.W., Xia, H., Chen, S.Y. and Roeck, G.D. (2010), "Structural damage identification for railway bridges based on train-induced bridge responses and sensitivity analysis", *J. Sound Vib.*, **330**, 757-770.
Zhang, J.H., Guo, P., Lin, J.W. and Wang, K. (2016), "A mathematical model for coupled vibration system of road vehicle and coupling effect analysis", *Appl. Math. Model.*, **40**, 1199-1217.
Zhu, X.Q., Law, S.S., Huang, L. and Zhu, S.Y. (2018), "Damage identification of supporting structures with a moving sensory system", *J. Sound. Vib.*, **415**, 111-127.